SUPPLEMENTARY INFORMATION

Allosteric opening of the polypeptide-binding site when an Hsp70 binds ATP

Ruifeng Qi, Evans Boateng Sarbeng, Qun Liu, Katherine Quynh Le, Xinping Xu, Hongya Xu, Jiao Yang, Jennifer Li Wong, Christina Vorvis, Wayne A. Hendrickson, Lei Zhou, and Qinglian Liu

Supplementary Figures 1-7

Supplementary Tables 1-2

Supplementary Figure 1.

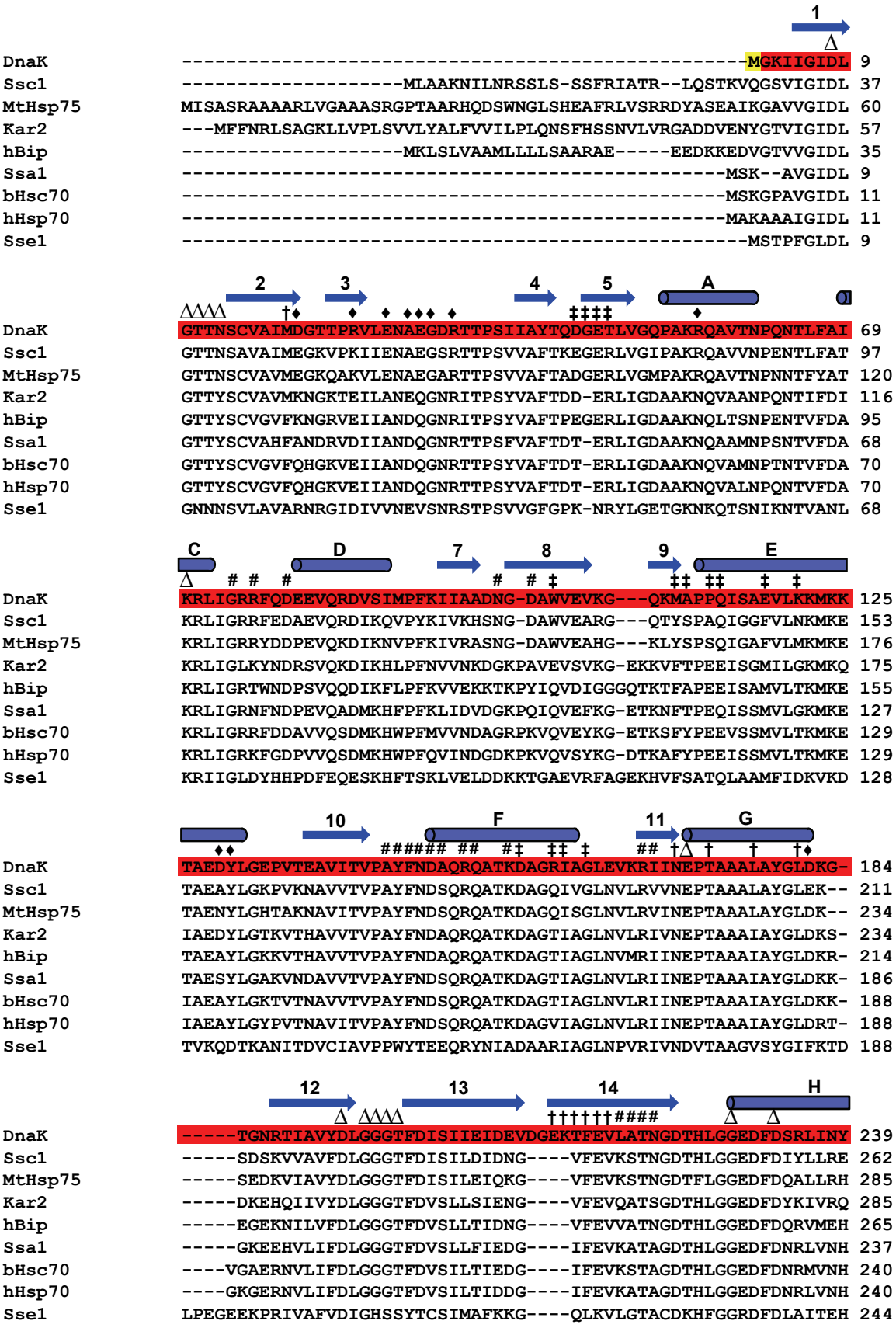

Supplementary Figure 1.

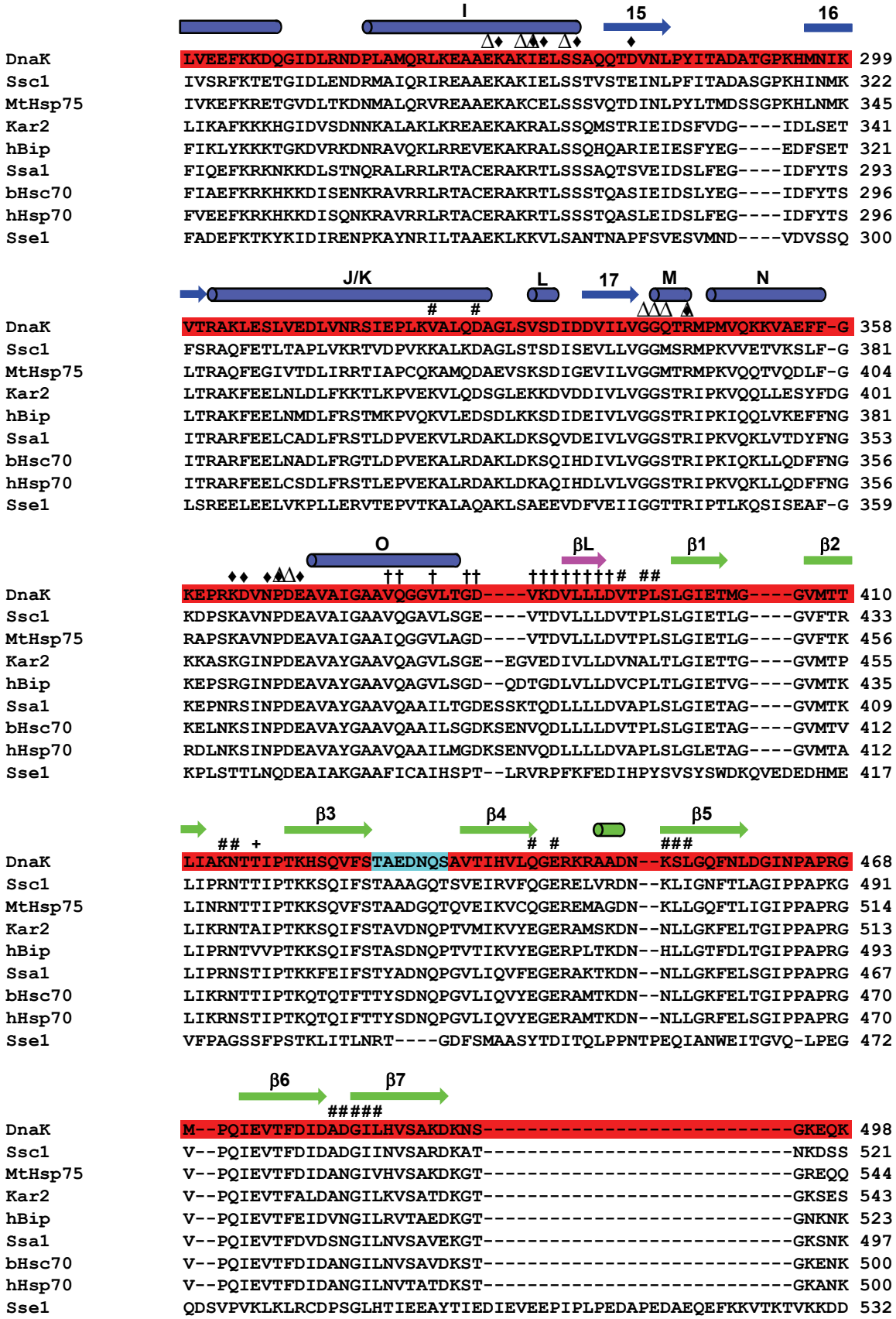

Supplementary Figure 1.

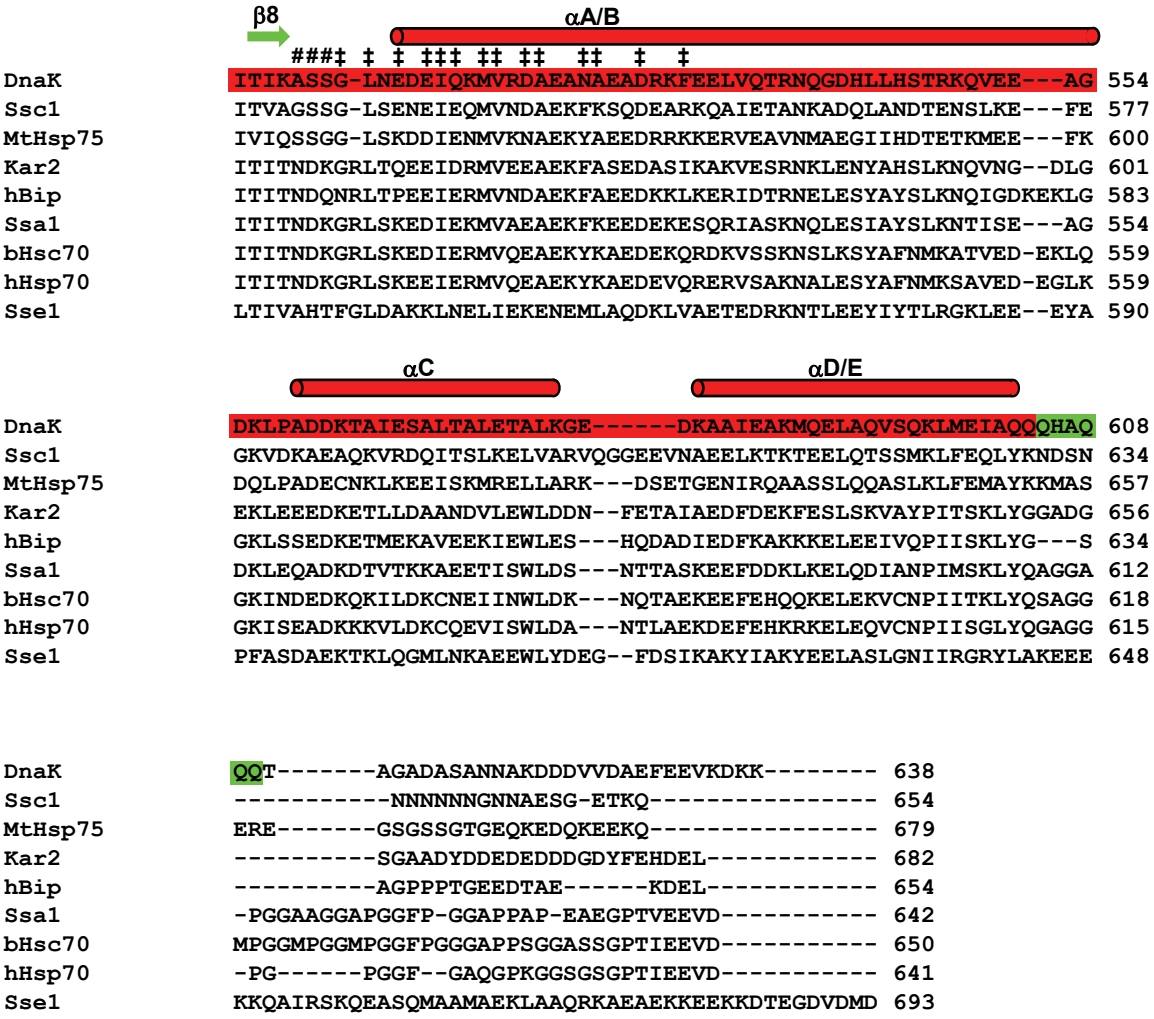

Supplementary Figure 1. Sequence alignment. The amino acid sequence of *E. coli* DnaK is aligned with the sequences of other selected Hsp70s and with yeast Hsp110 Sse1. The DnaK construct used in crystallization is from residue 1 to 610. The first 604 residues (highlighted in red) are ordered in both protomers, whereas the last 6 residues (highlighted in green) are not ordered in either protomer. $\mathcal{L}_{3,4}$, which is mutated to MGG ($\mathcal{L}'_{3,4}$), is highlighted in cyan; and residue 1, which is mutated to serine, is highlighted in yellow. Elements of secondary structure in the DnaK-ATP structure are specified by cylinders for helices and arrows for strands and labeled. The coloring of structural elements is: NBD (blue), Linker (purple), SBDβ (green) and SBDα (red). The contacting residues on the NBD-Linker, NBD-SBDβ, NBD-SBDα, and Linker-SBDβ interfaces are labeled with †, #, ‡, and +, respectively, on top of the sequence. NBD-NBD dimer-interface contacting residues are labeled with ♦, and ATP contacting residues are labeled with ∆.

Supplementary Figure 2.

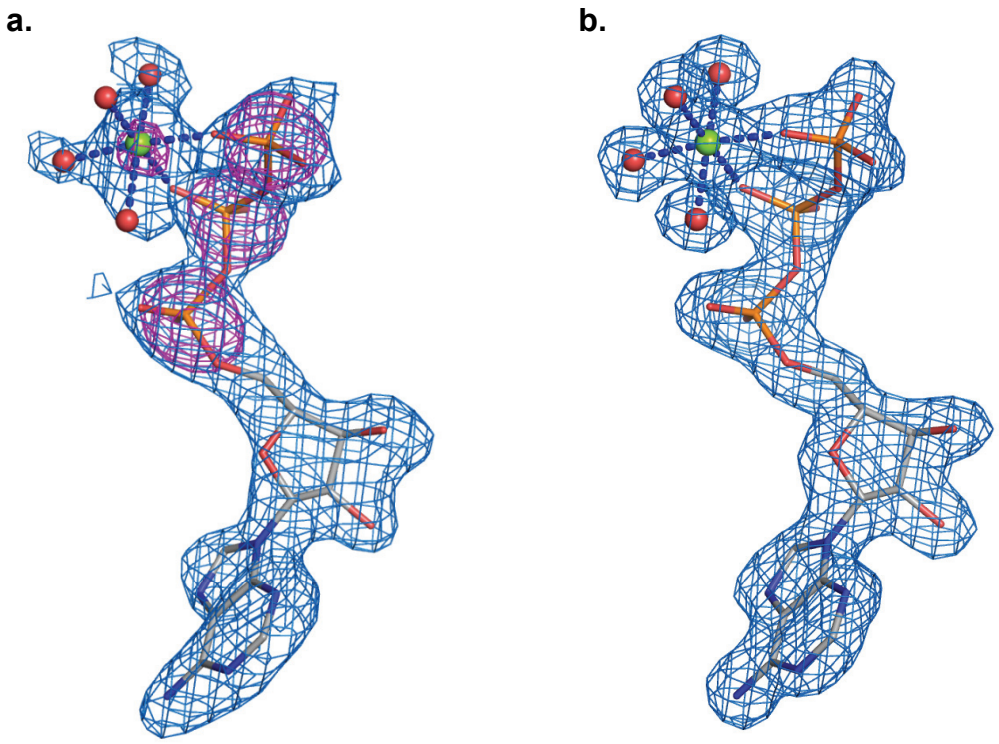

Supplementary Figure 2. Electron-density distributions for the ATP-Mg^{2+} molecule. **a**, SAD-phased experimental electron-density map at 2.3 Å resolution. Experimental phases based on the 5-crystal native-SAD data were improved by DM density modification, but without molecular averaging. The resulting mFo map is colored in marine and contoured at 1.8σ. The corresponding Bijvoet-difference Fourier synthesis is colored in magenta and contoured at 5σ to show the strong peaks for the phosphorus atoms of ATP as well as Mg^{2+} ion. **b**, Refined 2Fo-Fc electron-density map at 1.96 Å resolution (colored in marine and contoured at 1.8 σ). Both in **a** and in **b**, the ATP molecule is from protomer A, and the refined atomic model is drawn as color-coded sticks and balls: carbon (gray), nitrogen (blue), oxygen (red), phosporous (orange), magnesium (green). Note the octahedral coordination of the Mg^{2+} ion by oxygen atoms from four water molecules and the β and γ phosphate groups. Electron densities associated with the Mg^{2+}-ATP complex were selected with the 'covering' option in PyMOL (http://www.pymol.org).

Supplementary Figure 3.

a.

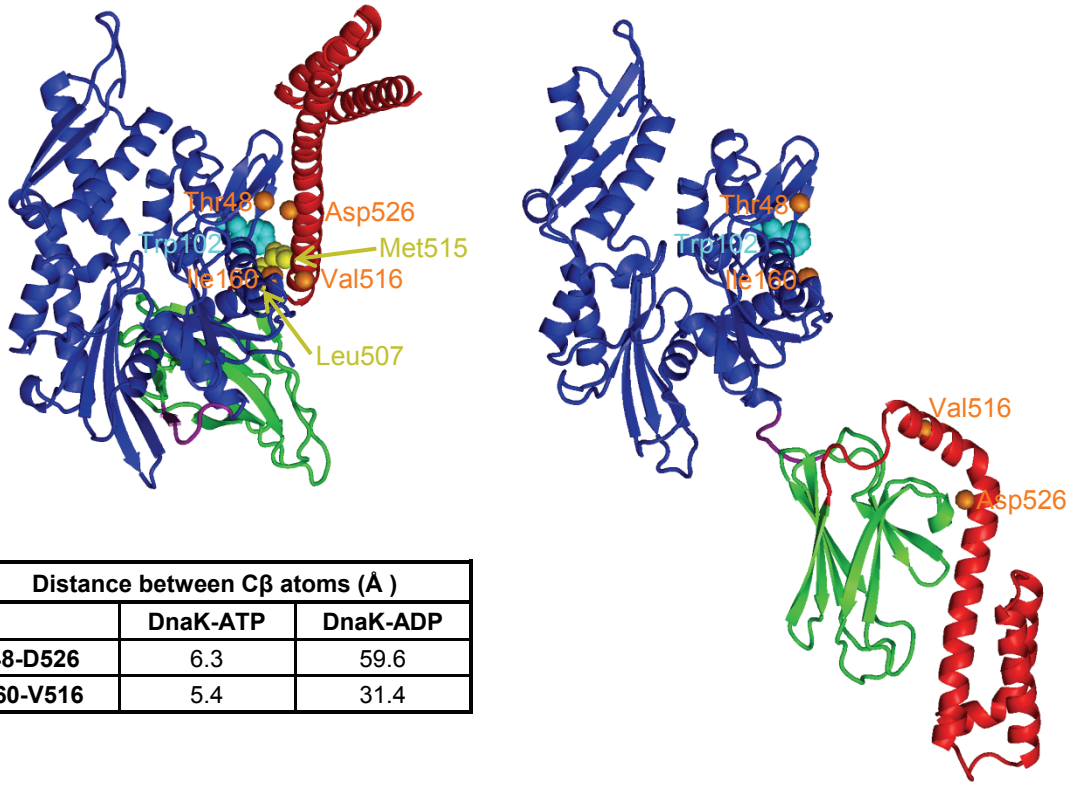

b.

Distance between Cβ atoms (Å)		
	DnaK-ATP	**DnaK-ADP**
T48-D526	6.3	59.6
I160-V516	5.4	31.4

c.

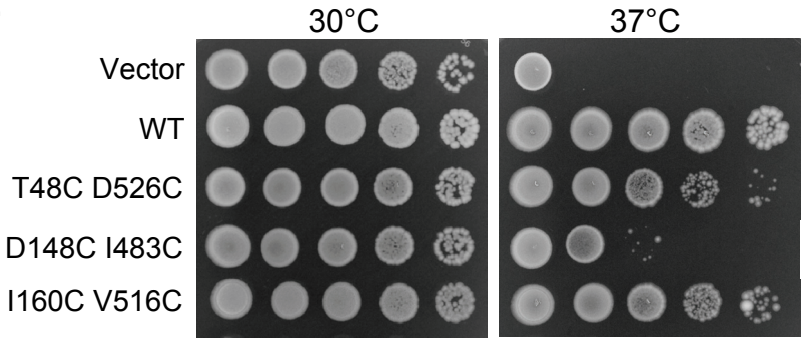

d.

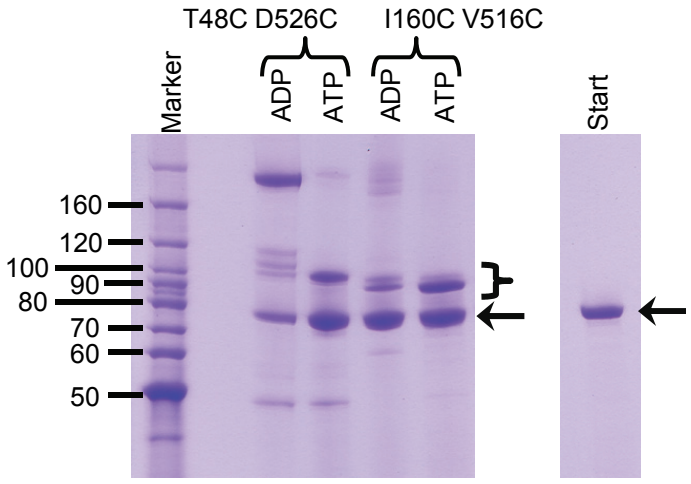

Supplementary Figure 3.

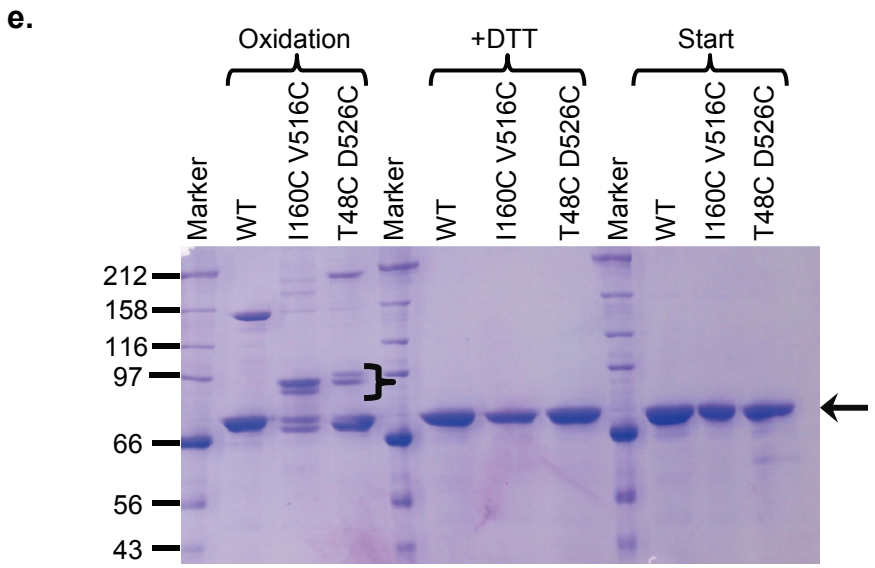

Supplementary Figure 3. Tests of the DnaK-ATP conformation using disulfide-bond formation. **a,** Positions of Trp102 and the residues selected for mutation to cysteine residues in the DnaK-ATP (left) and DnaK-ADP (right; PDB 2KHO) structures. Domain coloring is the same as **Fig. 1a**. Trp102 (cyan) and its interacting residues on SBDα, Leu507 and Met515 (yellow), are highlighted in sphere representation. Pairs of residues selected for mutation, Thr48-Asp526 and Ile160-Val516, are identified by orange balls. These residues are neighboring in the NBD-SBDα interface of DnaK-ATP structure (left) but far apart in the DnaK-ADP structure (right). **b,** Distances between the Cβ atoms of prospective pairs. **c,** Growth tests of double-cysteine mutants in DnaK. Assays were done the same way as for **Fig. 4b**. Chaperone function is largely intact for both DnaK-T48C D526C and DnaK-I160C V516C double-cysteine mutants. We also tested a pair of residues on the NBD-SBDβ interface of DnaK-ATP, Asp148 and Ile483; However, the DnaK-D148C I483C mutant abolished the function of DnaK; thus, we did not further pursue this mutant. **d,** Disulfide bond formation of the DnaK-T48C D526C and DnaK-I160C V516C proteins with overnight air oxidation. Purified DnaK protein ("start" lanes, indicated by arrows) runs between 70 to 80 kDa on SDS-PAGE. After oxidation, overnight in air at room temperature, both DnaK-T48C D526C and DnaK-I160C V516C proteins formed bands running at marker positions between 90 to 100 kDa (indicated by a bracket) specifically in the presence of ATP. The shifted positions are compatible with intramolecular disulfide-bond formations between T48C and D526C and between I160C and V516C for the respective proteins. In the presence of ADP, both proteins formed disulfide-bonded bands at marker positions corresponding to large molecular weights (>160 kDa, top panel); these bands are most likely due to intermolecular disulfide-bond formation. This is consistent with the observation that T48C and I160C are exposed on the surface of NBD in the DnaK-ADP structure, and thus are well positioned for forming intermolecular disulfide bonds. **e,** Chemical reduction of disulfide-bonded proteins. The double-cysteine proteins were oxidized in the presence of ATP as before, but here accelerated by adding copper phenanthroline. The addition of DTT after such oxidation restored the positions of protein bands to those of the starting materials, which is consistent with disulfide bonding as the basis for the ATP-selective shifts upon oxidation.

Supplementary Figure 4.

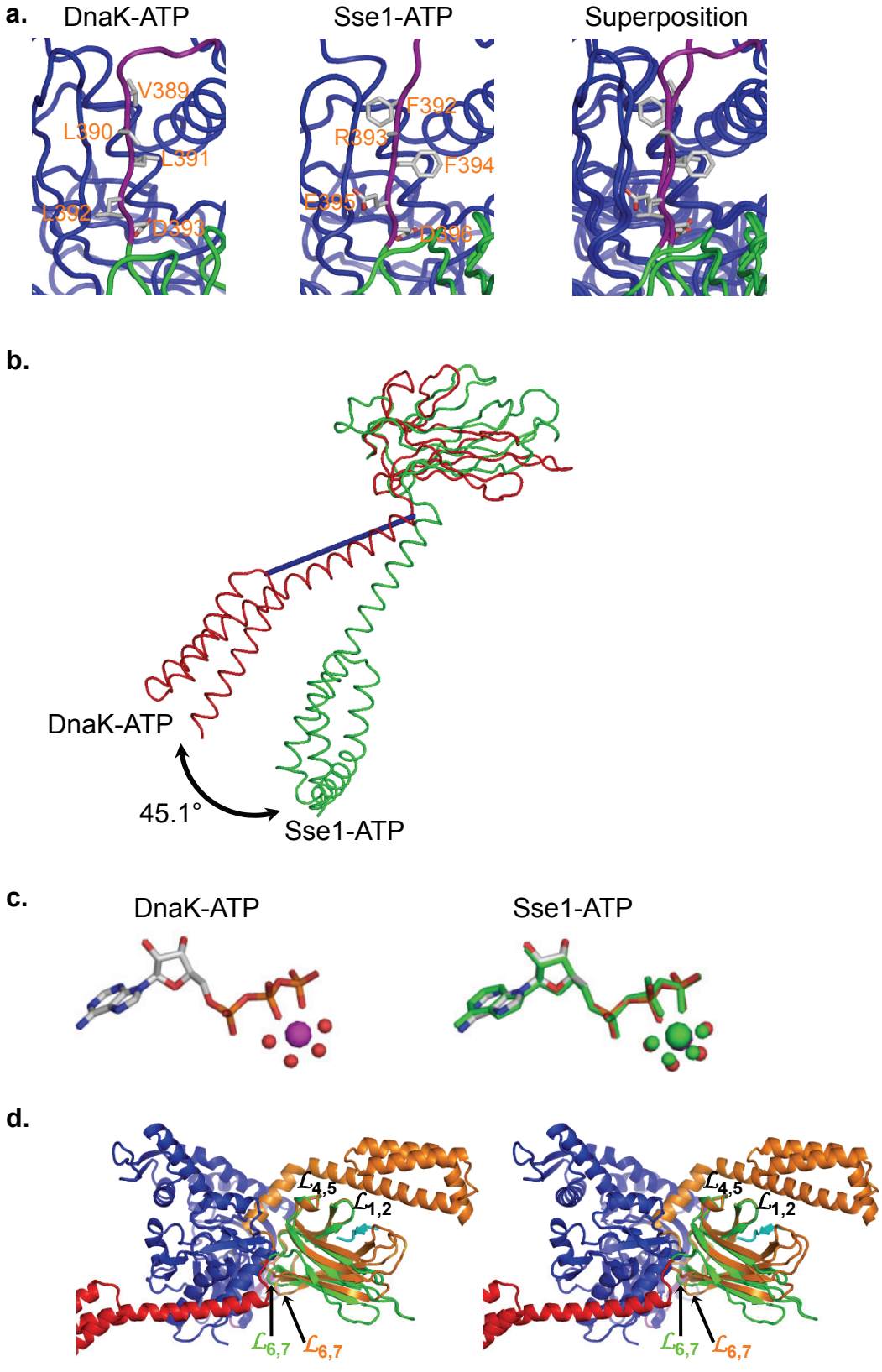

Supplementary Figure 4.

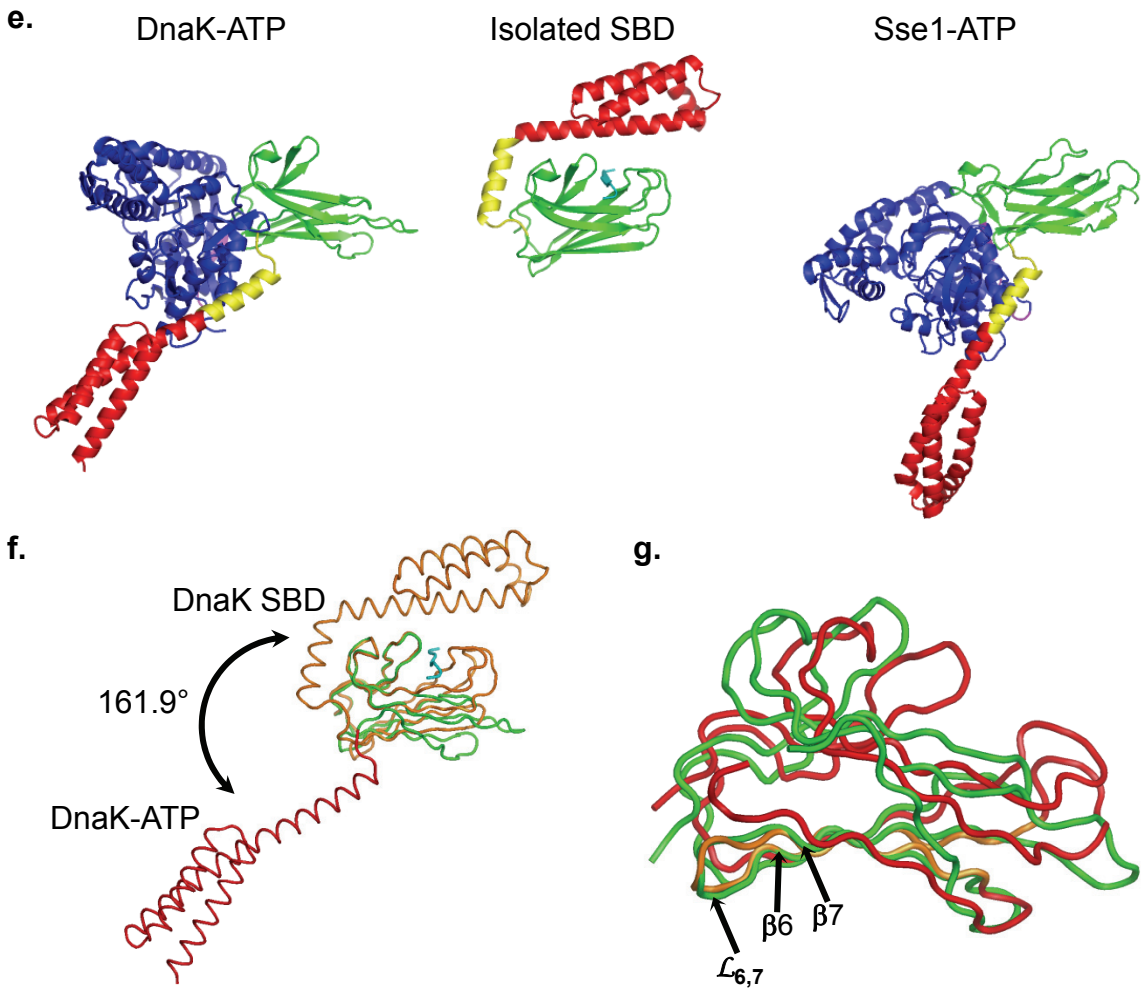

Supplementary Figure 4. Structural comparisons. **a**, Comparison of the Linker segments in the DnaK-ATP (left) and Sse1-ATP (middle; PDB 2QXL) structures. Domain coloring is the same as in **Fig. 1a**. The two structures are superimposed on the right. **b**, Superposition of SBDs from the DnaK-ATP (red) and Sse1-ATP (green) structures as based on comparable SBDβ Cα atoms. The rotation axis is shown as a blue rod. **c**, Comparison of the ATP molecules from the DnaK-ATP and Sse1-ATP structures. Left: ATP from DnaK-ATP (protomer A) is shown in stick representation with the associated Mg^{2+} ion shown as a purple ball and the coordinating water molecules shown as red balls. Right: Superposition of ATP molecule from DnaK-ATP as drawn on the left with that from Sse1-ATP (green). **d**, Superposition of DnaK-ATP and isolated DnaK SBD (PDB 1DKZ) in stereo drawings as based on Cα atoms in $\mathcal{L}_{1,2}$ and $\mathcal{L}_{4,5}$. The coloring of the DnaK-ATP structure is the same as in **Fig. 2b**. The isolated SBD is in orange, and the bound NR peptide is in cyan. **e,** Ribbon drawings of DnaK-ATP (left), isolated DnaK SBD (middle), and Sse1-ATP (right), respectively. Domain coloring is the same as **Fig. 1a** except that the first alpha helix of SBDα is colored in yellow. Peptide NR is in cyan. Orientations are based on superpositions of common SBDβ Cα atoms. **f**, Superposition, as in **d**, of SBDs from DnaK–ATP (green for SBDβ and red for SBDα) and isolated SBD (orange) based on the SBDβ Cα atoms. **g,** The SBDβs from the DnaK-ATP structure (green) and the isolated SBD structure (orange for the β6-$\mathcal{L}_{6,7}$-β7 segment and red for the rest) are superimposed based on the Cα atoms of β6-$\mathcal{L}_{6,7}$-β7, thus showing that the two β6-$\mathcal{L}_{6,7}$-β7 segments have almost identical conformations.

Supplementary Figure 5.

a.

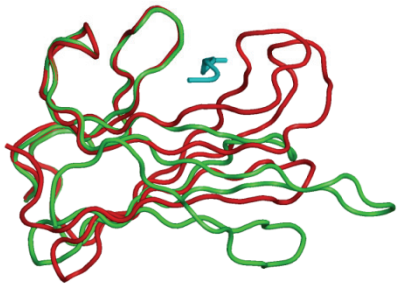

b.

c.

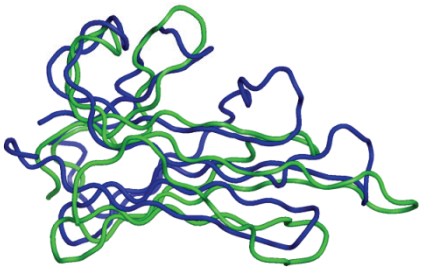

d.

Backbone conformation, φ(°), ψ(°)				
	DnaK-ATP	**DnaK-SBD (NR peptide)**	**SBDβ-empty (16#)**	**SBDβ-empty (20#)**
Gly461	-66.4, 168.6	83.5, 13.1	84.8, 42.2	174.7, -42.7
Gly468	-81.8, 126.6	79.8, 3.9	127.2, -41.6	70.4, 32.0

e.

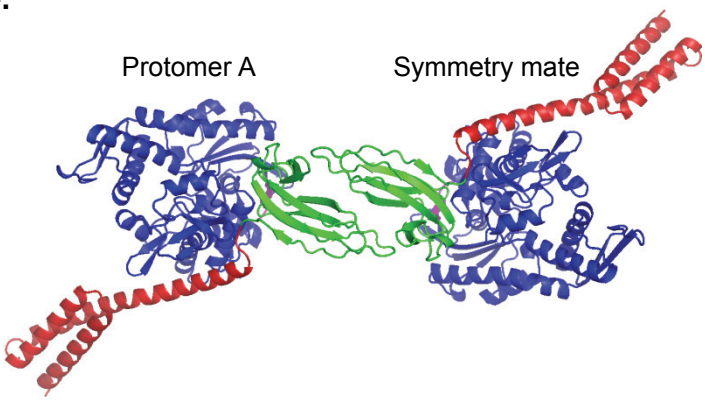

f.

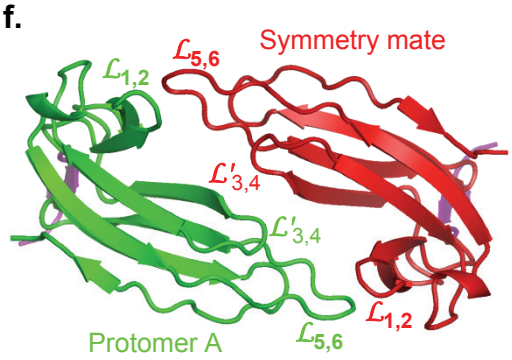

g.

Number of stable contacts within SBDβ				
Normalized covariance factor cutoff	**DnaK-ATP**	**DnaK-SBD (NR peptide)**	**DnaK-SBD (no peptide)**	**SBDβ-empty (20#)**
0.8	735	13	0	1
0.7	1528	67	5	10
0.6	2279	180	72	47

Supplementary Figure 5. SBDβ structure comparisons and crystal contacts. a, Superposition of SBDβs from the DnaK-ATP (green) and isolated DnaK SBD (red; PDB 1DKZ) as based on Cα atoms in $\mathcal{L}_{1,2}$ and $\mathcal{L}_{4,5}$. The bound NR peptide is in cyan. **b,** and **c,** Superposition of the SBDβs from the DnaK-ATP (green) and two models of the NMR structure of DnaK SBDβ without peptide substrates (SBD-empty; PDB 1DG4),16# (orange) and 20# (blue), respectively. Among all the 20 models of the NMR structure, 16# most closely resembles the isolated DnaK SBD crystal structure, whereas structure 20# most closely resembles the DnaK-ATP structure. **d,** Comparison of phi and psi conformational angles for Gly461 and Gly468. DnaK-SBD: the crystals structure of DnaK SBD in complex with NR peptide (PDB 1DKZ). SBD-empty: NMR structure of DnaK SBDβ (PDB 1DG4). **e**, Crystal contacts are formed between SBDβs in the DnaK-ATP structure. Crystal contacts between protomer A (left) and its symmetry mate (right) are shown. Domain coloring for DnaK molecules is the same as **Fig. 2b**. **f**, Details of the SBDβ crystal contacts shown in **e**. NBDs and SBDαs are not shown. Crystal contacts are formed between $\mathcal{L}_{1,2}$ and $\mathcal{L}_{5,6}$, and between the two $\mathcal{L}'_{3,4}$ loops. **g,** Comparison of stable contacts within SBDβ calculated based on molecular dynamic (MD) simulation analysis without consideration of crystal contacts and symmetry mates. The higher the normalized covariance factor, the more stable a contact is. The SBDβ in the DnaK-ATP structure has the greatest number of stable contacts; whereas the NMR structure without peptide substrate has the fewest number of stable contacts. Moreover, removing the bound peptide substrate from the isolated SBD structure, DnaK-SBD (no peptide), significantly reduced the number of stable contacts to close to the empty SBD structure solved by NMR.

Supplementary Figure 6.

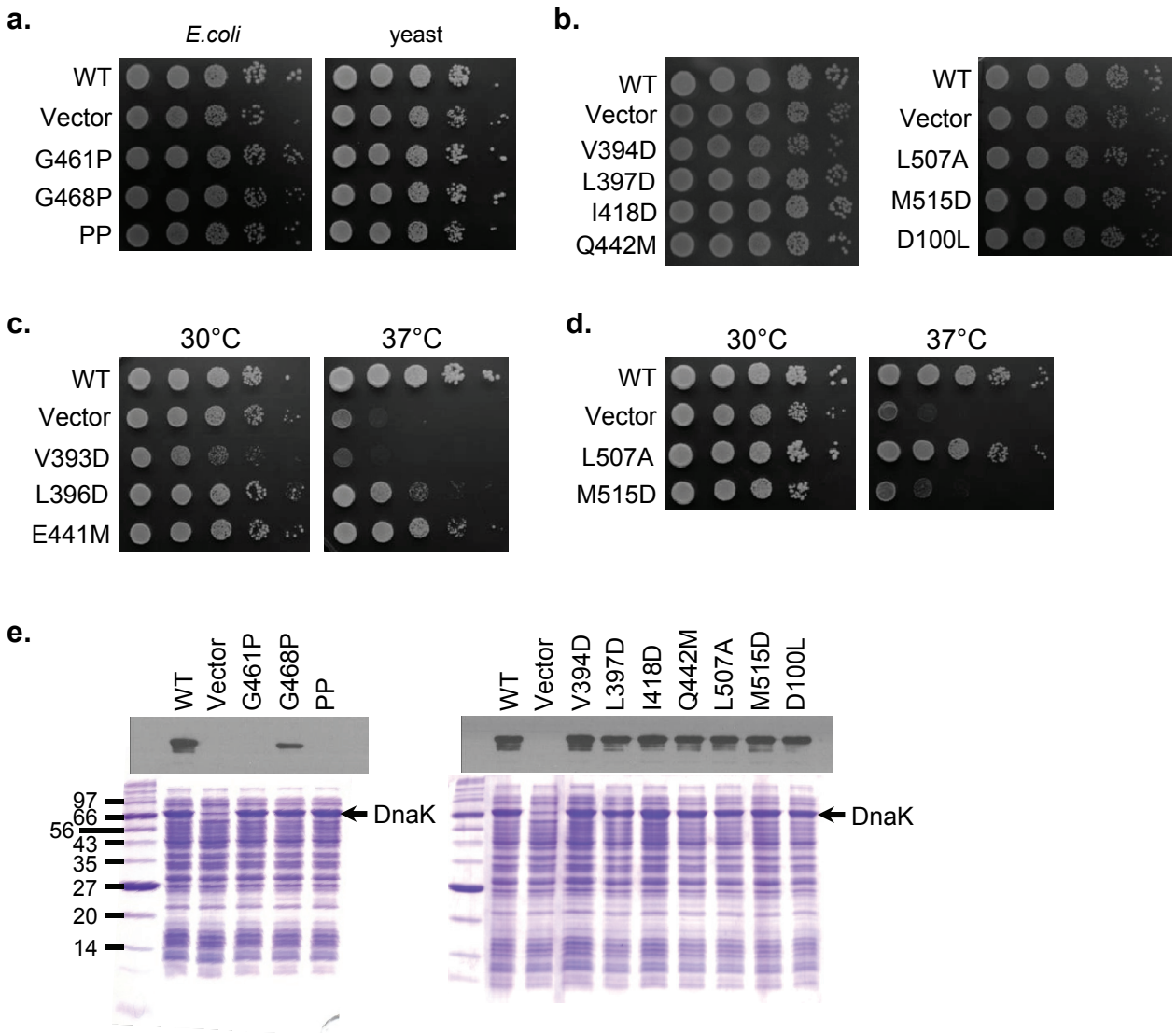

Supplementary Figure 6. Growth tests and expression levels of mutant DnaK proteins. **a** and **b**, Growth controls at permissive temperature, 30°C. **a**, Glycine mutations in both DnaK and Ssa1. **b**, Mutations on the inter-domain interfaces in DnaK. **c** and **d**, Growth tests for the interfacial mutants in yeast Ssa1. Growth at 30°C was used as controls. Residues Val393, Leu396, Glu441, Leu507 and Met515 in Ssa1 correspond to Val394, Leu397, Gln442, Leu507 and Met515 in DnaK. **c**, Mutants on the NBD-SBDβ interface; **d**, Mutants on the NBD-SBDα interface. **e,** Expression levels of mutant DnaK proteins. For each mutant construct, an equal amount of *E.coli* cells was loaded onto SDS PAGE. Top panels: Western-blot analysis with an anti-DnaK antibody, mAb 8E2/2 (Calbiochem), performed as described previously[23]. Bottom panels: SDS PAGE stained with Coomassie blue. The first lane on each gel is the molecular weight marker (labeled in kDa). For unknown reason, the DnaK antibody used in our assay does not recognize the G461P and PP mutants although SDS PAGE stained with Coomassie blue suggested that both expressed at similar level as the WT DnaK.

Supplementary Figure 7.

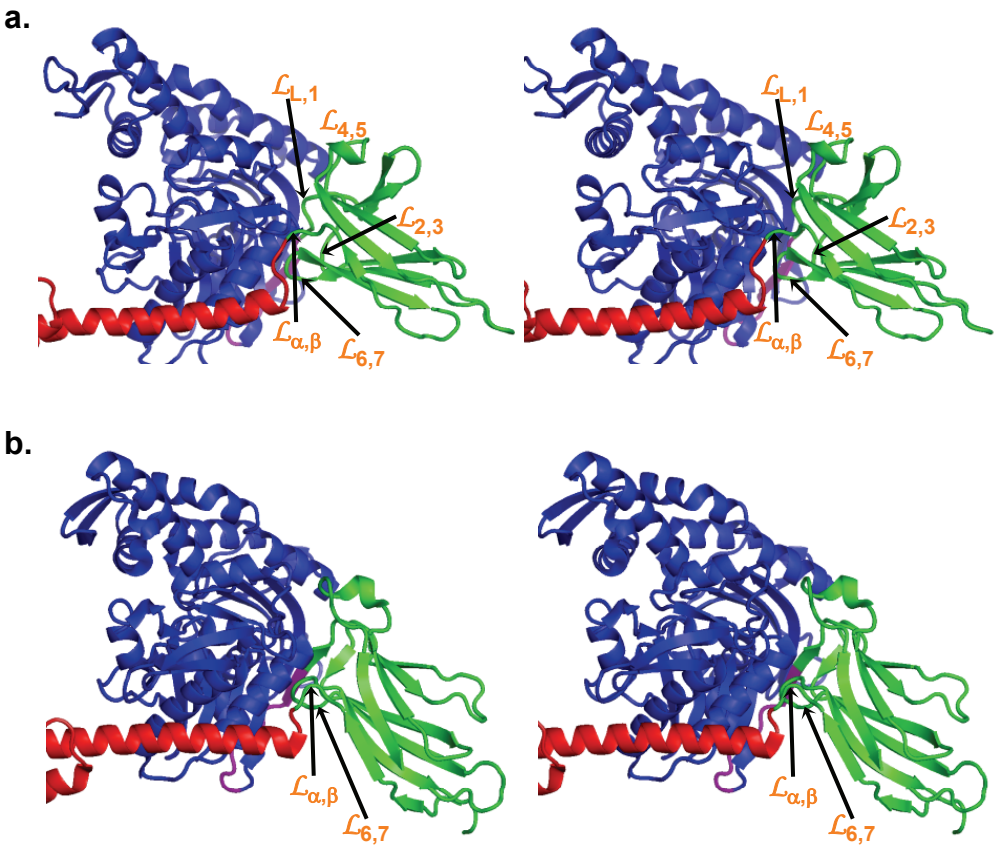

Supplementary Figure 7.

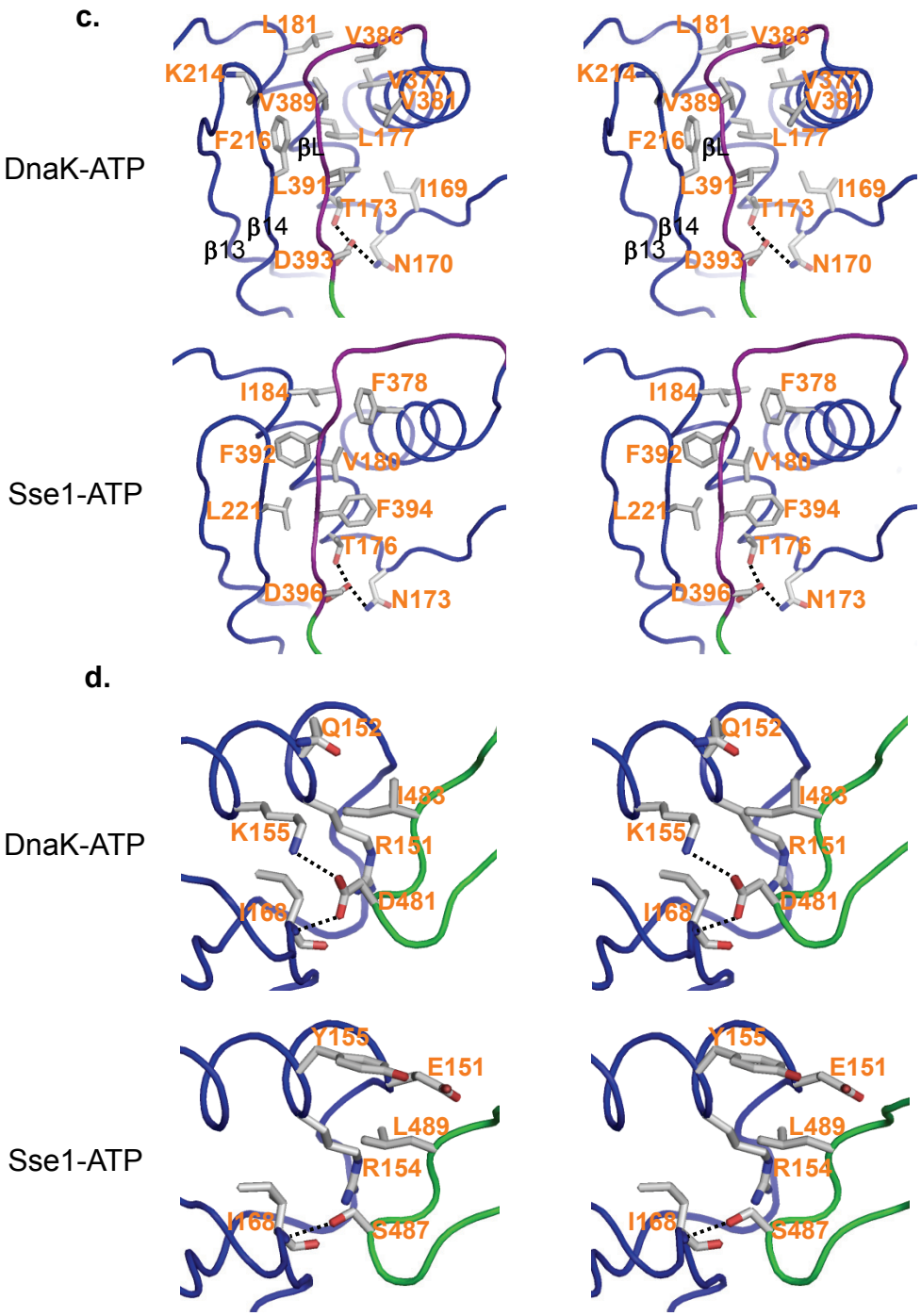

Supplementary Figure 7.

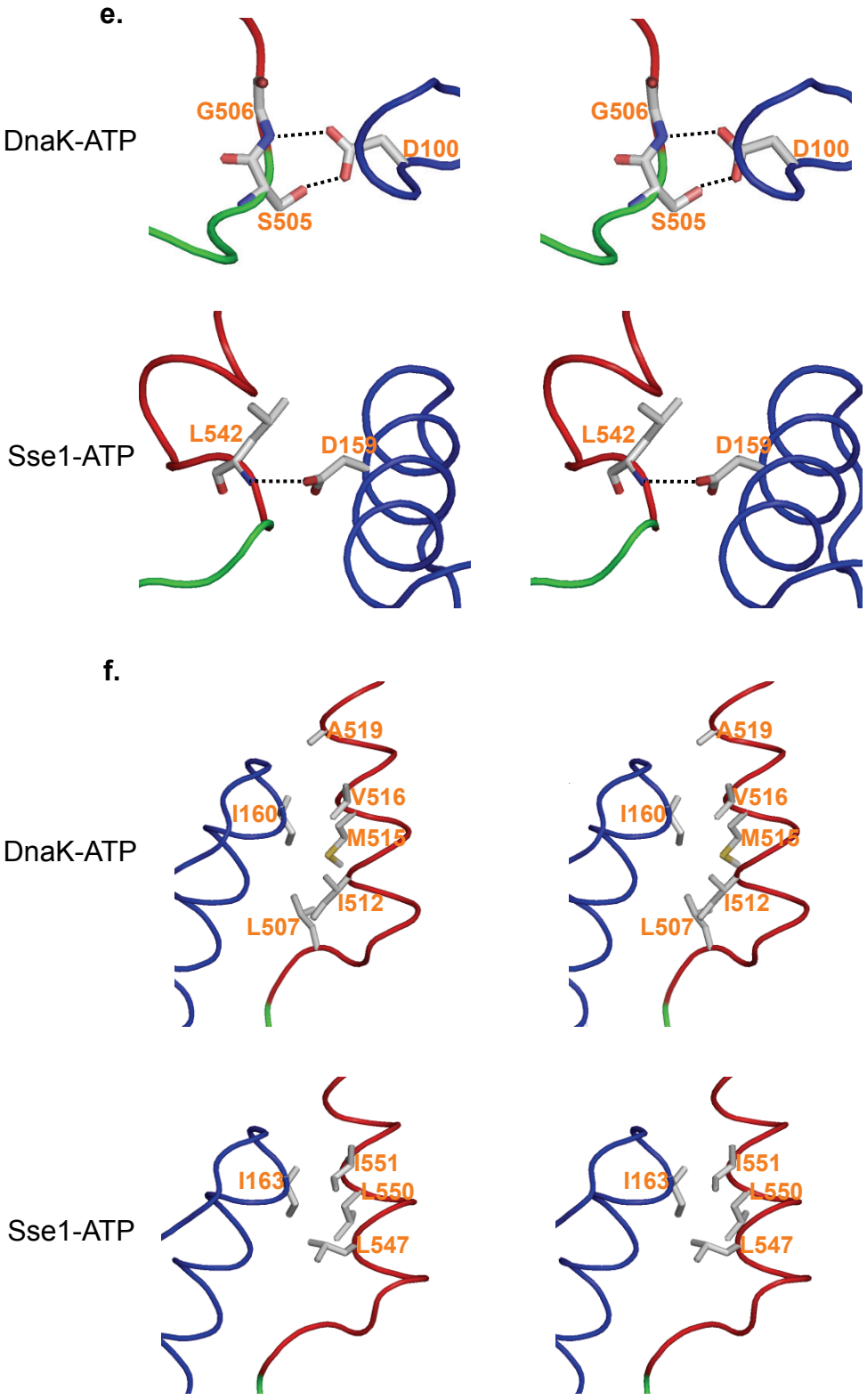

Supplementary Figure 7.

g. NBD-$\mathcal{L}_{L,1}$

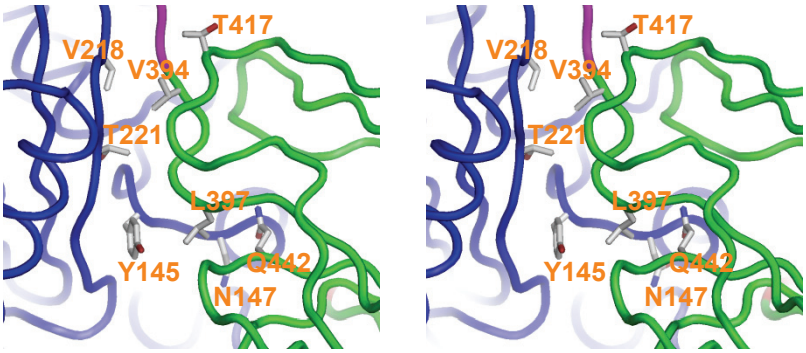

h. NBD-$\mathcal{L}_{2,3}$

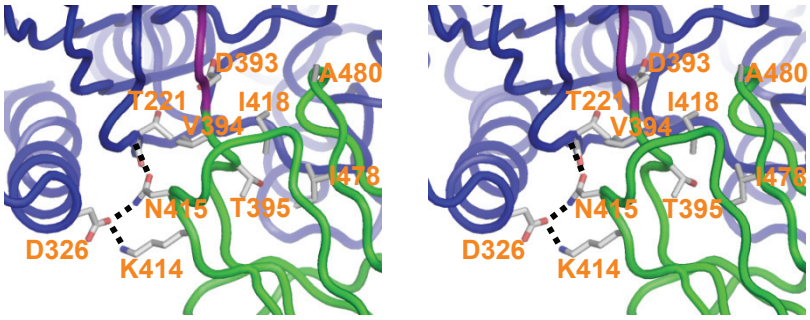

i. NBD-$\mathcal{L}_{4,5}$

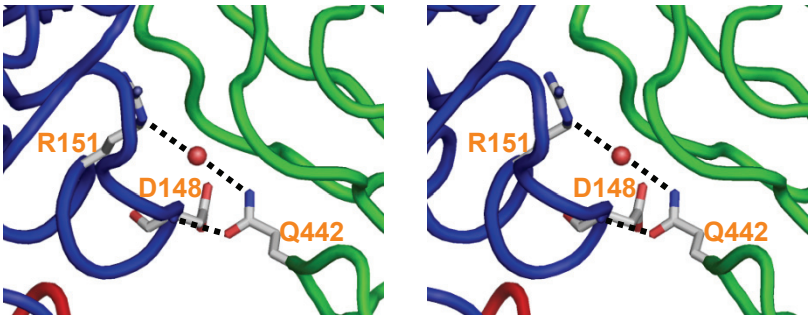

j. NBD-SBDα

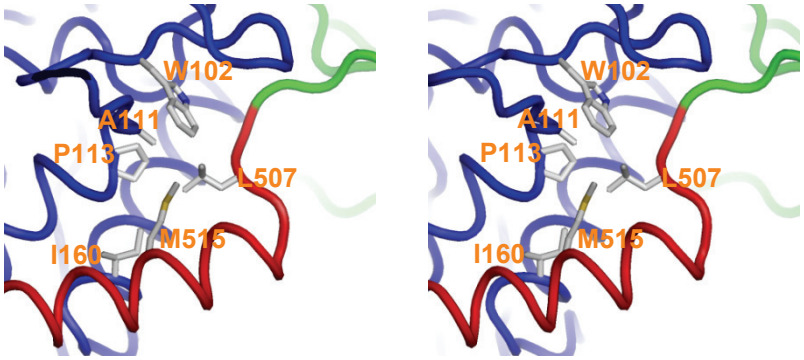

Supplementary Figure 7. Inter-domain contacts in the DnaK-ATP and Sse1-ATP structures. a and **b**, Overall comparison of the DnaK-ATP (**a**) and Sse1-ATP (**b**) structures in stereo drawings. Orientations in **a** and **b** are based on superpositions of Cα atoms of NBD. Domain coloring is the same as in **Fig. 1a**. The SBDβ loops that form direct contacts with NBD are labeled in both structures: $\mathcal{L}_{L,1}$, $\mathcal{L}_{2,3}$, $\mathcal{L}_{4,5}$, $\mathcal{L}_{6,7}$, and $\mathcal{L}_{\alpha,\beta}$ in the DnaK-ATP structure; only $\mathcal{L}_{6,7}$, and $\mathcal{L}_{\alpha,\beta}$ in the Sse1-ATP structure. **c-f,** Stereo drawings of the similar NBD-SBD contacts shared in the DnaK-ATP and Sse1-ATP structures. Top panels are from the DnaK-ATP structure, and bottom panels are from the Sse1-ATP structure. Side chains are shown for residues that are hydrogen-bonded or in van der Waals contact across the interfaces. **c**, The NBD-Linker interface. Val389, Leu391 and Asp393 on the Linker mediate almost identical interactions with NBD in both structures. **d**, The contact between NBD and $\mathcal{L}_{6,7}$ from SBDβ. Two conserved residues, Asp481 and Ile483 in DnaK (Ser487 and Leu489 in Sse1), form close contacts with NBD in both structures, but with changes in their counterparts on the NBD. **e**, The NBD-$\mathcal{L}_{\alpha,\beta}$ contact. Asp100 forms hydrogen bonds with $\mathcal{L}_{\alpha,\beta}$ in the DnaK-ATP structure, whereas in the Sse1-ATP structure, it is Asp159, which is homologous to Asp156 rather than to Asp100, that forms hydrogen bond with $\mathcal{L}_{\alpha,\beta}$. **f**, The contact between NBD and SBDα. Ile160 in DnaK and Ile163 in Sse1 mediate similar hydrophobic interactions. **g-j,** Stereo drawings of the NBD-SBD contacts that are especially distinctive in DnaK-ATP as compared to Sse1-ATP**.** Corresponding mono figures are in **Fig. 6a**.

Supplementary Table 1. Buried surface area and shape complementarity on the interfaces

	Sse1-ATP		DnaK-ATP	
	Buried Surface area (Å²)	**Shape complementarity**	**Buried Surface area (Å²)**	**Shape complementarity**
Linker-rest	1407	0.730	1358	0.614
Linker-NBD	1196	0.734	1208	0.683
Linker-SBD	255	0.802	288	0.508
NBD-SBD	2594	0.684	2828	0.635
NBD-SBDβ	1427	0.667	1739	0.593
NBD-SBDα	1216	0.705	1170	0.702
Dimer interface	1976	0.471	3065	0.708
NBD-NBD'	562	0.522	1408	0.727
NBD(A)-SBD(B)	734	0.437	796	0.707
NBD(B)-SBD(A)	714	0.475	817	0.681

Sse1: NBD, 3-385; Linker, 386-396; SBD, 397-652; SBDα, 397-540; SBDβ, 541-652.
DnaK: NBD, 3-384; Linker, 385-393; SBD, 394-600; SBDα, 394-501; SBDβ, 502-600.

Supplementary Table 2. Peptide substrate binding affinities. Affinity for a model peptide, F-NR, was determined for each DnaK protein using a fluorescence anisotropy assay. Standard errors are shown for six sets of binding data from two different purifications (n=6).

	K_d (μM)
WT	**1.38±0.06**
V394D	**1.37±0.08**
L397D	**0.94±0.04**
I418D	**3.18±0.22**
Q442M	**1.31±0.05**
L507A	**1.46±0.08**
M515D	**1.02±0.06**